International Journal of Heat and Mass Transfer 52 (2009) 1991–2001

Contents lists available at ScienceDirect

International Journal of Heat and Mass Transfer

journal homepage: www.elsevier.com/locate/ijhmt

Augmentation of heat transfer from a solid cylinder wrapped with a porous layer

S. Bhattacharyya *, A.K. Singh

Department of Mathematics, Indian Institute of Technology, Kharagpur 721 302, India

ARTICLE INFO

Article history:
Received 5 January 2008
Received in revised form 6 August 2008
Available online 16 December 2008

Keywords:
Porous foam
Convective heat transfer
Pressure correction

ABSTRACT

In the present study, the heat transfer from a porous wrapped solid cylinder is considered. The heated cylinder is placed horizontally and is subjected to a uniform cross-flow. The aim is to investigate the heat transfer augmentation through the inclusion of a porous wrapper. The porous layer is of foam material with high porosity and thermal conductivity. The mixed convection is studied for different values of flow parameters such as Reynolds number (based on radius of solid cylinder and stream velocity), Grashof number, permeability and thermal conductivity of the porous material. The optimal value of porous layer thickness for heat transfer augmentation and its dependence on other properties of the porous foam is obtained. The flow field is analyzed through a single domain approach in which the porous layer is considered as a pseudo-fluid and the composite region as a continuum. A pressure correction based iterative algorithm is used for computation. Our results show that a thin porous wrapper of high thermal conductivity can enhance the rate of heat transfer substantially. Periodic vortex shedding is observed from the porous shrouded solid cylinder for high values of Reynolds number. The frequency of oscillation due to vortex shedding is dampened due to the presence of the porous coating. Beyond a critical value of the porous layer thickness, the average rate of heat transfer approaches asymptotically the value corresponding to the case where the heated cylinder is embedded in an unbounded porous medium.

1. Introduction

The use of a porous media leading to insulation/augmentation of heat transfer is widespread in industrial applications such as the insulation of heat pipes, electronic cooling, heat exchangers, food processing, catalytic reactors, refrigeration, air cooling and thermal energy storage devices. The study of heat transfer from or to a cylinder sheathed by a porous layer also has applications in human clothing (Sobera et al. [1]). Foam materials have been introduced recently in heat transfer enhancement technology. Foam is a highly permeable porous medium with high thermal conductivity, which enables a considerable reduced pressure drop for the through flow. The thermophysical properties of aluminum-based foam material has been discussed by Pack et al. [2]. Recently, Strautman et al. [3] conducted an experimental study on convective heat transfer enhancement by bounding a layer of porous carbon foam to a solid metal substrate and allowing fluid to flow across the foam surface. The layer of porous aluminum or carbon foam are found to be an efficient technology for heat transfer enhancement [2,3]. Saada et al. [4] conducted a numerical study on natural convection about a horizontal heated cylinder with a porous or fibrous coating.

The wake behind a solid circular cylinder is complicated due to the onset of vortex shedding. It is well established now that the wake becomes periodic for Reynolds number beyond 40. The vortex shedding from the cylinder leads to a large fluctuation in pressure forces in a direction transverse to the flow, which causes a structural vibration, acoustic noise or resonance. When a bluff body is subjected to vortex shedding, the heat transfer characteristics of the body changes considerably. The forced convection characteristics from a heated circular cylinder was studied by Chang and Sa [5]. It was found that the heat transfer rate improved considerably for unsteady flow as compared to that obtained from the steady flow. In the mixed convection regime owing to the buoyancy effect added to the viscous phenomena, the heat transfer and vortex shedding became more complicated. The wake structure behind a heated horizontal cylinder exposed to a cross-flow has been considered by Kieft et al. [6]. The inclusion of a porous wrapper is expected to delay the onset of vortex shedding from the porous wrapped solid cylinder. One of our objectives in the present work is to investigate the effect of vortex shedding on heat transfer from the porous shrouded solid cylinder in mixed convection regime. The heat flux from the solid cylinder should enhance when the vortex shedding sets in.

The theoretical and experimental study on heat transfer in porous media has drawn the attention of several researchers over the years. Several authors have reported the natural convection in porous media using the Darcy law to describe the fluid flow. A

* Corresponding author.
E-mail address: somnath@maths.iitkgp.ernet.in (S. Bhattacharyya).

0017-9310/$ - see front matter © 2008 Elsevier Ltd. All rights reserved.
doi:10.1016/j.ijheatmasstransfer.2008.08.041

Nomenclature

c_p	specific heat
Da	darcy number
E_f	heat transfer efficiency factor, $\overline{Nu_{av}}/(\overline{Nu_{av}})_f$
e_p	non-dimensional porous layer thickness, e_p^*/R
g	gravitational acceleration
h	heat transfer coefficient
g	gravity acceleration
Gr	Grashof number, $4g\beta(T_s - T_\infty)R^3/\nu^2$
k	permeability
Nu	local Nusselt number
Nu_{av}	mean Nusselt number
p	pressure
Pr	Prandtl number, ν/α
r	radial coordinate, r^*/R
R	cylinder radius
Ra	Rayleigh number, $g\beta(T_s - T_\infty)R^3/\alpha\nu$
Rc	thermal conductivity ratio, κ_e/κ
Re	Reynolds number, $2RU_\infty/\nu$
Ri	Richardson number, Gr/Re^2
T	temperature
t	time
u	radial velocity component
v	cross-radial velocity component

Greek symbols

α	thermal diffusivity, $\kappa/\rho c_p$
β	coefficient of thermal expansion
κ	thermal conductivity of clear fluid
$\bar{\kappa}$	thermal conductivity of solid matrix
κ_e	effective thermal conductivity of porous material, $\kappa_e = \varepsilon\kappa + (1-\varepsilon)\bar{\kappa}$
ε	porosity
μ	dynamic viscosity
ν	kinematic viscosity, μ/ρ
ρ	clear fluid density
θ	cross-radial coordinate

Subscripts

∞	free stream
f	fluid

comprehensive review on forced and mixed convection in a porous media can be found in the recent books by Ingham and Pop [7] and Nield and Bejan [8]. Pop et al. [9] analyzed analytically the transient natural convection in a horizontal concentric annulus filled with a porous medium. The mixed convection in a horizontal annulus filled with a porous medium is studied by Khanafer and Chamka [10]. There, they investigated the effect of Rayleigh number on the heat transfer from the inner heated cylinder in mixed convection. However, the Darcy law to describe the flow in the highly porous foam region may not be applicable and heat transfer due to convection may not be negligible within the porous region. We have considered the flow field for high values of Reynolds number, for which the applicability of Darcy law is questionable.

The present work deals with the flow and heat transfer from a porous layer coated solid cylinder placed horizontally in a cross-flow due to a uniform stream. The cylinder is assumed to be heated with a uniform surface temperature. We consider the porous layer to be made up of foam material with high porosity and high effective thermal conductivity, so that it produces an enhancement in the net heat transfer. The buoyancy induced flow characteristics and heat transfer is analyzed. The main motivation of this study is to estimate the optimal porous layer thickness for heat transfer augmentation and to investigate its dependence on the thermal conductivity and permeability of the porous layer. Beside this, in several practical contexts the control of vortex shedding plays an important role. A thin porous coating may significantly damp the shedding frequency. The present study shows that the frequency of vortex shedding is reduced considerably through the inclusion of a porous wrapper.

To simulate the composite systems of fluid and porous media, it is necessary to solve simultaneously the Brinkman equation in the porous media and the Navier–Stokes equations in the clear fluids along with a suitable matching condition at the interface. The implementation of the interface condition (Beavers and Joseph [11] and Saffman [12]) is complicated as it contains material dependent parameters whose value must be determined empirically. In the single domain formulation [13,14, and the references cited there in], the two sets of equations for the fluid and the porous regions are combined into one set by introducing a binary parameter. In this approach, the values from both sides of the interface are used to obtain solutions, and therefore the matching of variable values are inherent in the formulation itself.

A pressure correction based iterative algorithm is used for computation. Flow field and heat transfer are computed to investigate the optimal thickness of the porous layer for heat transfer augmentation in both natural convection and mixed convection cases.

2. Governing equation

We consider that a solid cylinder kept at a constant temperature T_s, which is higher than the ambient temperature T_∞, is coated with a thin porous layer of non-dimensional thickness e_p. The porous wrapped solid cylinder is placed horizontally (with respect to g) and is subjected to a uniform cross-flow U_∞ (refer Fig. 1). The porous layer has a uniform porosity ε and permeability k. The radius of the cylinder R and free stream velocity U_∞ are taken to be the characteristic length and velocity scale, respectively. The Brinkman model is used to express the governing equation inside the porous layer and the Navier–Stokes equations to describe the fluid flow outside the porous layer. The single domain approach,

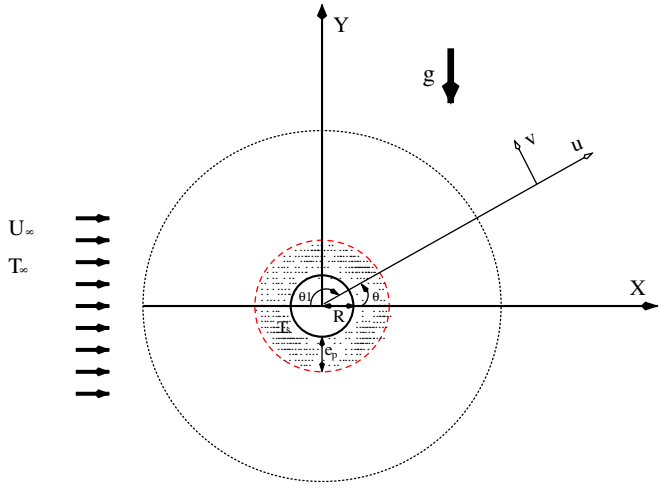

Fig. 1. Sketch of the flow configuration.

where a single set of equations are used to describe the fluid flow in the porous layer as well as the fluid region with appropriate switching terms, is adopted in the present analysis. The fluid velocity $\vec{V}$ inside the porous region is related to the fluid velocity $\vec{v}$ through the Dupuit–Forchheimer relationship as $\vec{v} = \varepsilon\vec{V}$, [8], where ε is the porosity. The equation governing the unsteady laminar flow through and around the porous layer in the non-dimensional form can be expressed as:

$$\frac{1}{r}\frac{\partial(ru)}{\partial r} + \frac{1}{r}\frac{\partial v}{\partial\theta} = 0, \tag{1}$$

$$\begin{aligned}&\frac{1}{\varepsilon}\frac{\partial u}{\partial t} + \frac{1}{\varepsilon^2}\left(\frac{v}{r}\frac{\partial u}{\partial\theta} + u\frac{\partial u}{\partial r} - \frac{v^2}{r}\right)\\ &= -\frac{\partial p}{\partial r} + \frac{2}{Re}\left(\frac{\partial^2 u}{\partial r^2} + \frac{1}{r}\frac{\partial u}{\partial r} + \frac{1}{r^2}\frac{\partial^2 u}{\partial\theta^2} - \frac{2}{r^2}\frac{\partial v}{\partial\theta} - \frac{u}{r^2}\right)\\ &\quad - \frac{2B}{ReDa}u + \frac{Gr}{Re^2}T\sin\theta,\end{aligned} \tag{2}$$

$$\begin{aligned}&\frac{1}{\varepsilon}\frac{\partial v}{\partial t} + \frac{1}{\varepsilon^2}\left(\frac{v}{r}\frac{\partial v}{\partial\theta} + u\frac{\partial v}{\partial r} - \frac{uv}{r}\right)\\ &= -\frac{1}{r}\frac{\partial p}{\partial\theta} + \frac{2}{Re}\left(\frac{\partial^2 v}{\partial r^2} + \frac{1}{r}\frac{\partial v}{\partial r} + \frac{1}{r^2}\frac{\partial^2 v}{\partial\theta^2} + \frac{2}{r^2}\frac{\partial u}{\partial\theta} - \frac{v}{r^2}\right) - \frac{2B}{ReDa}v + \frac{Gr}{Re^2}T\cos\theta,\end{aligned} \tag{3}$$

$$\frac{\partial T}{\partial t} + \left(\frac{v}{r}\frac{\partial T}{\partial\theta} + u\frac{\partial T}{\partial r}\right) = \frac{2Rc}{RePr}\left(\frac{\partial^2 T}{\partial r^2} + \frac{1}{r}\frac{\partial T}{\partial r} + \frac{1}{r^2}\frac{\partial^2 T}{\partial\theta^2}\right). \tag{4}$$

In the clear fluid region the Darcy number tends to infinity with $\varepsilon = 1$ and the thermal conductivity ratio (Rc) between the porous layer and clear fluid is equal to unity. The binary parameter $B = 0$ in clear fluid region and $B = 1$ in porous zone. The usual Boussineque approximation of neglecting the density variation due to heating in all terms except the buoyancy force term is made.

The dimensionless variable are defined as:

$$\begin{aligned}&u = u^*/U_\infty, \quad v = v^*/U_\infty, \quad t = U_\infty t^*/R, \; p = p^*/(\rho U_\infty^2),\\ &T = (T^* - T_\infty)/(T_s - T_\infty).\end{aligned} \tag{5}$$

The variable with superscript * denotes dimensional variables. The governing equations (2)–(4) are subjected to the following boundary conditions:

Along the upstream boundary ($\pi/2 \leqslant \theta \leqslant 3\pi/2$):

$$u = \cos\theta, \quad v = -\sin\theta, \quad T = 0. \tag{6}$$

Along the downstream boundary:

$$\frac{\partial u}{\partial r} = 0, \quad \frac{\partial v}{\partial r} = 0, \quad \frac{\partial T}{\partial r} = 0. \tag{7}$$

On the surface of the solid cylinder: ($r = 1$)

$$u = 0, \quad v = 0, \quad T = 1. \tag{8}$$

For the case of natural convection, we have scaled the velocity components by (α/R), consequently pressure is scale by $\rho(\alpha/R)^2$. The governing equations within the porous layer and in clear fluid region are the same as described in Saada et al. [4].

It may be noted that in the present formulation, no boundary condition is required at the interface. The local Nusselt number is evaluated at the wall of the cylinder in order to quantify heat transfer with respect to the influential parameters. It is define by:

$$Nu = -Rc\left(\frac{\partial T}{\partial r}\right)_{r=1}, \tag{9}$$

Nu_{av} is defined as the mean Nusselt number obtained as

$$Nu_{av} = \frac{1}{2\pi}\int_0^{2\pi} Nu\, d\theta, \tag{10}$$

and $\overline{Nu_{av}}$ is the time average of Nu_{av}, over a complete shedding cycle when the wake is time periodic.

3. Numerical method

A pressure correction-based iterative algorithm, SIMPLE (Fletcher [15]), is used to compute the governing equations. We now provide a brief description of the algorithm. The governing equations are integrated over a control volume in staggard grid arrangements. The control volume formulation ensures conservation of momentum and energy as well as the continuity of fluxes. In the Staggered grid arrangement, velocity components are stored at the midpoints of each cell sides to which they are normal and the scalar variable, such as pressure and temperature are stored at the center of the cell. The convective terms at any interface of the control volume are estimated by a linear interpolation between two grid-point neighbors on either side of the interface. The diffusion terms are discretized through a second order, central difference scheme. Thus, the discretization of the space derivatives is second order accurate. A first order implicit scheme is used to discretized the time derivative. The resulting algebraic equations are solved through a block elimination method due to Varga [16].

The pressure links between continuity, momentum and temperature is accomplished by transforming the continuity equation into a Poisson equation for pressure. This Poisson equation implements a pressure correction for a divergent velocity field. The pressure correction equation is solved using the successive-under-relaxation technique with the under-relaxation factor chosen as 0.7. With the corrected pressure, velocity and temperature fields are updated. The iteration process in each time step is continued until the divergence in each cell is below a preassigned small quantity ($\epsilon = 10^{-5}$).

A sharp change of thermophysical properties, such as the permeability, porosity and thermal conductivity occurs along the

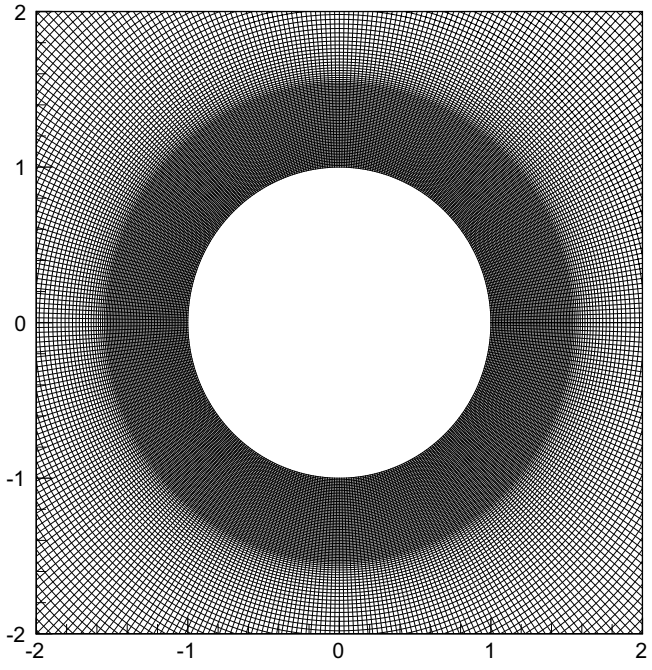

Fig. 2. Grid distribution around the cylinder for 400 × 260 grid.

fluid–porous interface. A harmonic mean formulation is used to handle such jump of the parameter values.

Since the velocity and temperature field near the solid cylinder and the fluid–porous interface vary more rapidly than elsewhere, a non-uniform grid distribution along the r-direction and uniform grid distribution along θ-direction is incorporated in the computation domain (see Fig. 2). We made a grid independence study by considering three sets of non-uniform grids namely, 400×260 and 300×224, with first and second number being the total number of grid points in θ- and r-directions, respectively. For the coarse grid, the minimum value of grid size along r-direction, i.e., $\delta r = 0.01$, whereas, for dense grid $\delta r = 0.005$. The $\delta\theta$ value is taken to be 0.02095 for coarse grid and 0.01366 for dense grid. The grid independence study is shown in Fig. 3a, where we computed the local Nusselt number for natural convection case and compared with the results due to Saada et al. [4]. The corresponding maximum percentage difference between the grid 460×291 and 400×260 is 0.7544. The maximum percentage difference between 460×291 and 300×224 is 3.7430. We find from the above that the grids 400×260 is optimal. The outer boundary for the present computation is placed at $20R$ from the center of the cylinder at $Re = 40$. This distance has been increased with the increase of Reynolds number.

In the present study, the computations are started either from rest or from the converged solution relating to lower Reynolds number. The time step is taken to be 0.001. After a short transition state, the flow either approaches to a steady state or unsteady time-periodic, depending on the Reynolds number and other flow parameters. The steady flow or the time periodic flow is independent of the initial conditions for the present range of Reynolds number.

To check the validity of our numerical method, we have compared our results for the natural convection case with the porous layer thickness, $e_p = 2$ with those of Saada et al. [4]. We found an excellent agreement of our results for local Nusselt number and the heat transfer efficiency factor $(E_f = \overline{Nu_{av}}/(\overline{Nu_{av}})_f)$ with Saada et al. [4], Fig. 3a and b. We have compared our results for $e_p = 0$ case with those of Badr [17] when forced convection $(Ri = 0)$ and Kieft et al. [6] when mixed convection is considered. Our results are in excellent agreement with those of the above published results (Fig. 4a and b).

4. Results and discussion

The flow and thermal field are governed by the physical parameters, such as the Darcy number (Da), porosity (ϵ), Reynolds number (Re), Grashof number (Gr), and the geometrical parameter e_p, which measures the non-dimensional thickness of the porous layer. To understand the heat transfer enhancement characteristics of different porous materials, we carried out a parametric study in which we fixed the fluid properties such as, viscosity, density and varied the permeability, porosity, thermal conductivity and the porous layer thickness. The flow field and heat transfer is then analyzed for different values of porous layer thickness (e_p) for moderate values of Reynolds number, $40 \leqslant Re \leqslant 200$ and Grashof number, $Gr = 10^4$ or 10^5 such that the Richardson number $(Ri = Gr/Re^2)$ assumes values greater than one as well as less than one. The Richardson number measures the relative importance of the forced and buoyant effects. The Prandtl number (Pr) for the clear fluid is taken to be 0.72 and the porosity (ε) is considered 0.9 for all the calculations.

4.1. Flow and thermal fields

When a bluff body (non-streamlined) is placed in a uniform stream of fluid, two separated shear layers are formed, one on each side of the body, the vorticity of the two layers being opposite. For the case of a solid cylinder wrapped with a porous layer, the strength of the separated shear layers are reduced and the length of the wake also reduces with the increase of the porous layer thickness. The wake behind a solid circular cylinder is steady for Reynolds number up to 40. Beyond this Reynolds number, vortex shedding behind the cylinder sets in and the wake becomes periodic. It is expected that with the inclusion of the porous layer, the development of the periodic wake will occur at a higher Reynolds number. The wake behind the porous wrapped cylinder is found to be steady at Reynolds number 80 for both the values of Darcy number (k/R^2) namely, $Da = 10^{-3}$ and $Da = 10^{-5}$. The form of the isotherms for steady mixed convection flow with $Gr = 10^5$ and $Re = 80$ is presented in Fig. 5. The isotherm for the natural convection case where $Gr = 10^5$ is also presented in Fig. 6 for $Da = 10^{-3}$ and $Da = 10^{-5}$. In natural convection, the isotherms form ring-like structure around the heated cylinder (see Fig. 6). A thermal plume develops vertically and the thermal field shows symmetry about the vertical axis, $y = 0$. When the cylinder is subjected to a cross-flow with Reynolds number 80, the flow field remains steady but the symmetry pattern is destroyed and the thermal plume is slanted. Results show that heat transfer within the porous layer is mostly dominated by conduction for lower range of Re at low Darcy number. A strong thermal boundary layer forms along the interface between the porous and fluid region. The convection effect is dominating on the outward side of this layer,

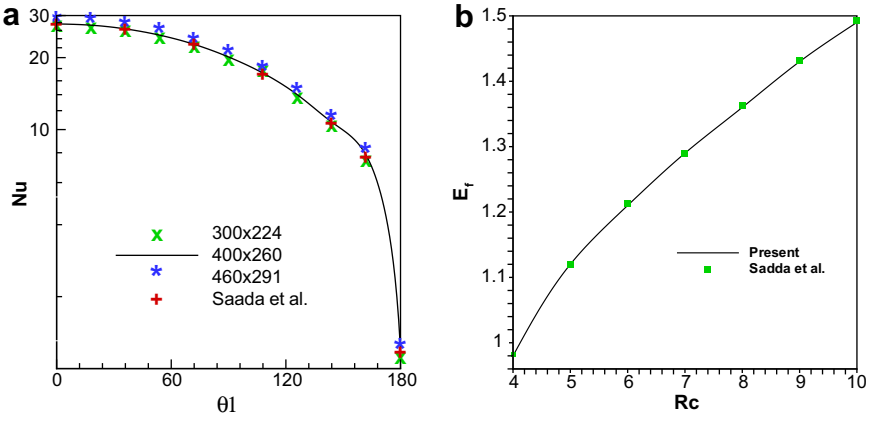

Fig. 3. Comparison of our results for natural convection with Saada et al. [4] for $e_p = 2$ when $Da = 4 \times 10^{-5}$, $Ra = 0.125 \times 10^8$ and $Pr = 0.7$. (a) Local Nusselt number (Nu) along the surface of the solid cylinder at $Rc = 1$. The effect of grid size is also shown; and (b) effect of thermal conductivity (Rc) on the heat transfer efficiency factor (E_f).

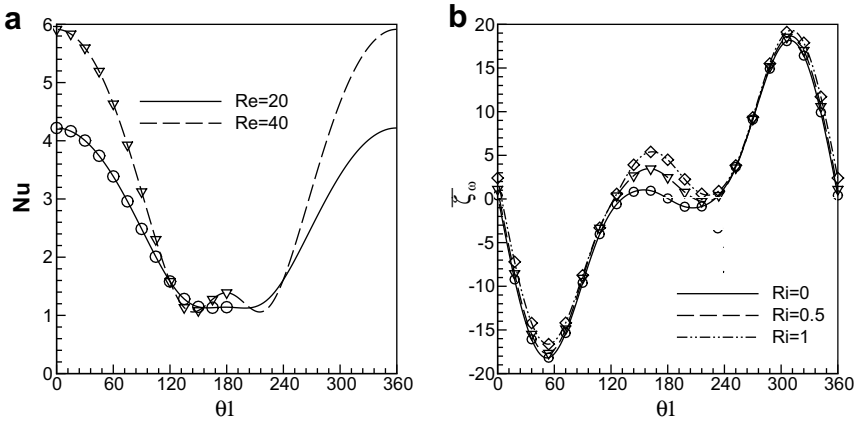

Fig. 4. Comparison of our results when no porous layer is considered ($e_p = 0$) for (a) local Nusselt number (Nu) for forced convection at different Re (=20, 40) (symbols correspond to the result due to Badr [17], ▽ for Re = 40 and ○ for Re = 20); (b) period-averaged surface vorticity ($\overline{\zeta_\omega}$) in mixed convection (symbols correspond to result due to Kieft et al. [6] at Re = 75, ○ for Ri = 0, ▽ for Ri = 0.5 and ◇ for Ri = 1).

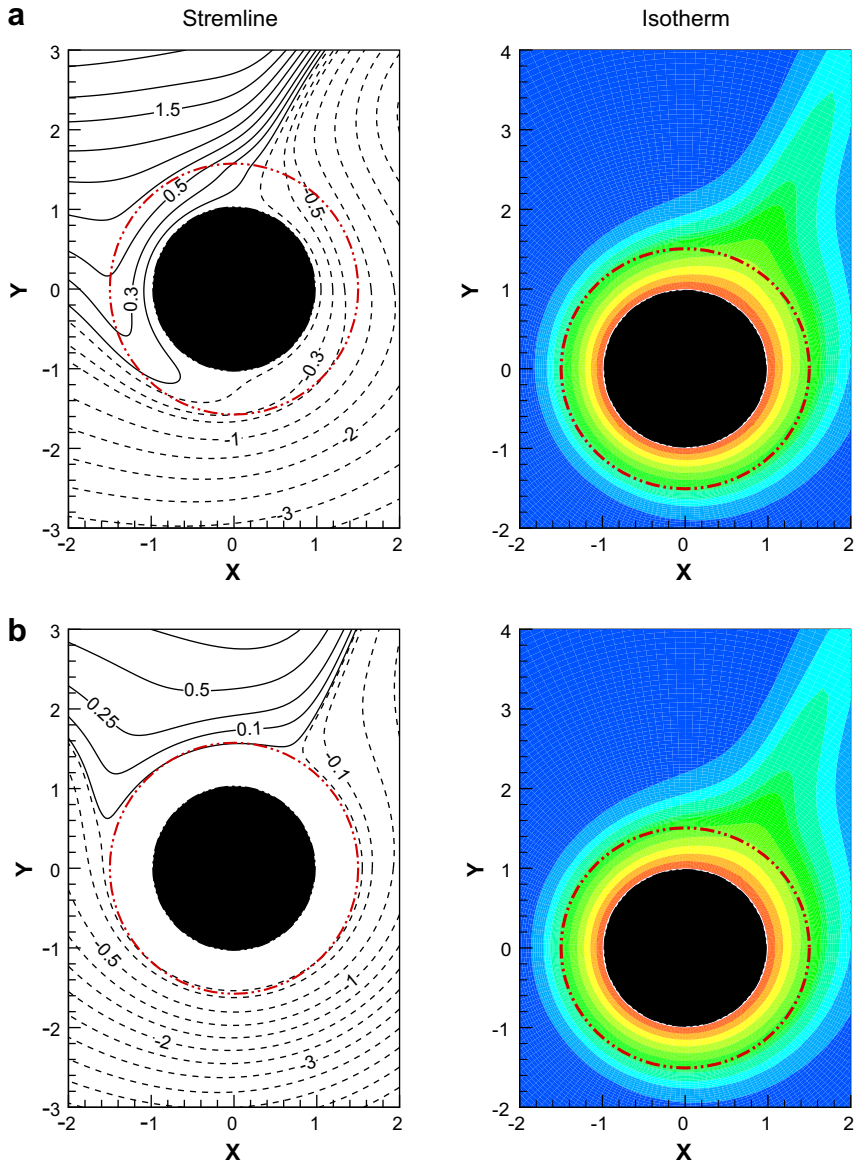

Fig. 5. Streamlines and Isotherm in mixed convection with $e_p = 0.5$, Re = 80, $Gr = 10^5$ and $Rc = 10$, (a) $Da = 10^{-3}$; (b) $Da = 10^{-5}$.

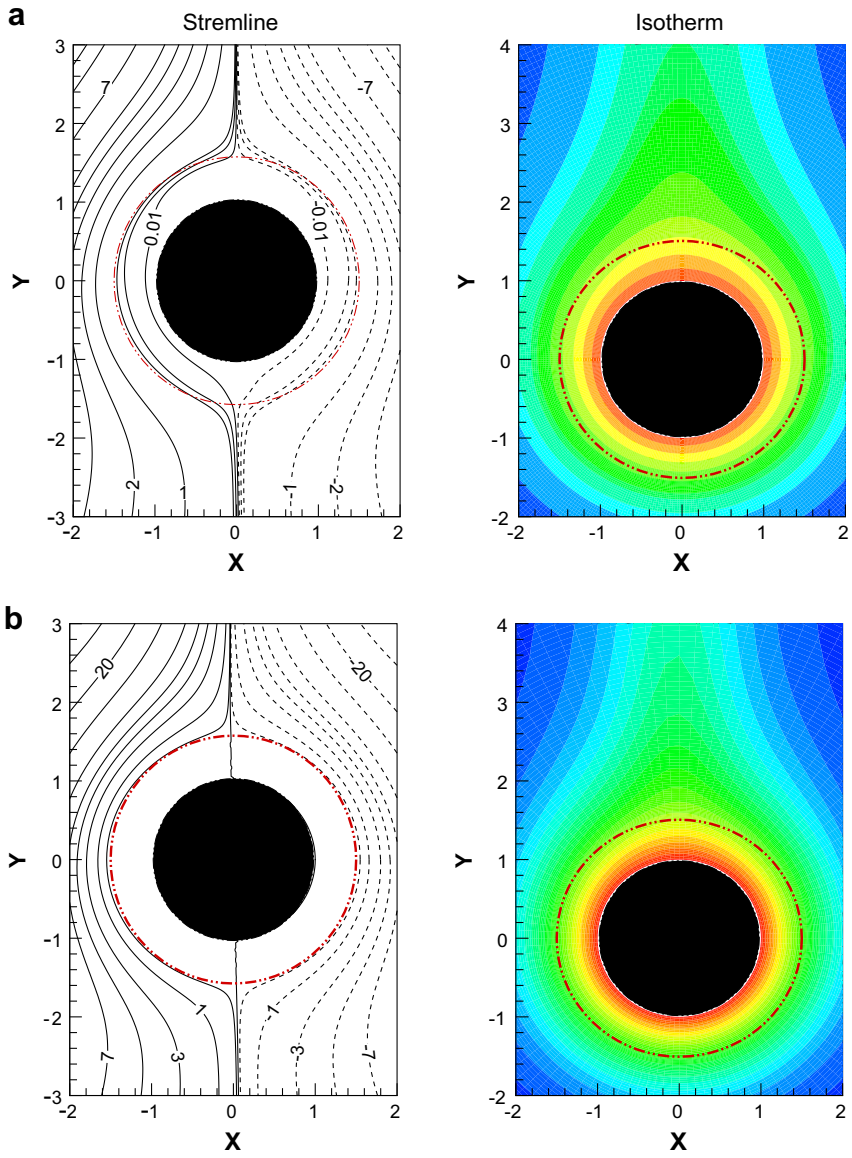

Fig. 6. Streamlines and Isotherm in natural convection with $e_p = 0.5$, $Gr = 10^5$ and $Rc = 10$, (a) $Da = 10^{-3}$; (b) $Da = 10^{-5}$.

but heat transfer is mostly through diffusion in the inward side. Vorticity also partly diffuses into the porous layer and a weak layer along the internal side of the fluid–porous interface forms. The streamline pattern show that the fluid penetration into the porous layer occurs for higher value of Darcy number ($Da = 10^{-3}$). Penetration of fluid into the porous zone is stronger at higher values of Reynolds number (80).

In order to check the time dependency of the flow field, we present the time evolution of the lift coefficient for $Re = 200$ and $Gr = 10^5$ ($Ri = 2.5$) at different values of the porous layer thickness (e_p). The results show that the flow field attains periodicity after a short transition for all values of the porous layer thickness considered ($e_p \leqslant 2$). Fig. 7 shows that the amplitude of oscillation of C_L is increased with the increase of e_p. We find that the time average lift experienced by the cylinder is negative (downwards). For flow with prominent buoyancy effect (i.e., $Ri \geqslant 1$), the increased heat produces a stronger negative vortex and the cylinder experiences a downwards lift.

Vortex shedding is a phenomenon which occurs when fluid flows past a bluff body. Boundary layer of slow moving viscous fluids is formed along the outer surface of the body and, because it is not streamlined and the fluid flow cannot follow the contours of the body, it becomes detached and roll up into vortices. For Reynolds number beyond 40, the shear layers exhibit Kelvin–Helmeholtz instability and an alternate vortex shedding is observed for the case of a solid cylinder. This periodic vortex shedding induces an oscillation in the surface forces. The buoyancy creates an imbalance in the strength of the separated shear layers and thus the negative vortices shed into the wake are stronger than the positive vortices (Kieft et al. [6]). It is expected that with the inclusion of porous layer the development of the periodic wake will be delayed with respect to the Reynolds number. Our results show that the lift and drag coefficients (not presented here) oscillate even when the cylinder is wrapped with a porous layer. The critical value of Re for the transition from steady to periodic wake increases with the increase of the porous layer thickness. The critical Reynolds number for the onset of vortex shedding becomes higher with the reduction of porous layer permeability (k).

The Strouhal number (St) measures the vortex shedding frequency and is obtained through the frequency of oscillation of

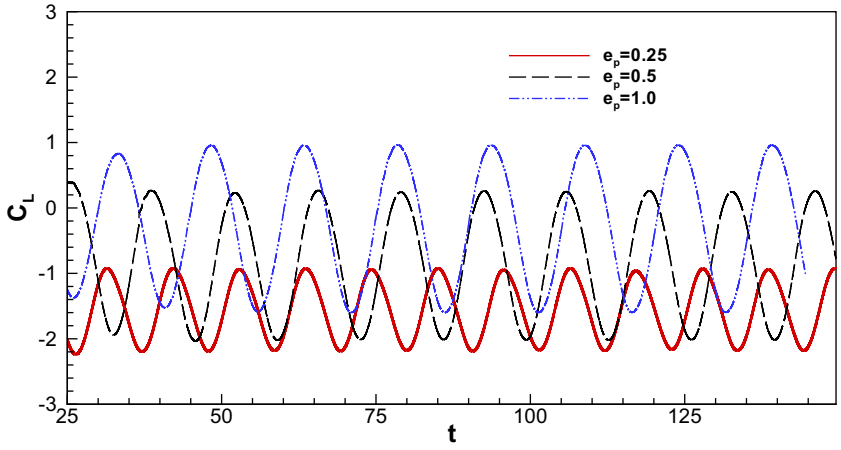

Fig. 7. Time evolution of lift coefficient (C_L) when $Da = 10^{-5}$, $Gr = 10^5$ and $Rc = 10$ for different e_p.

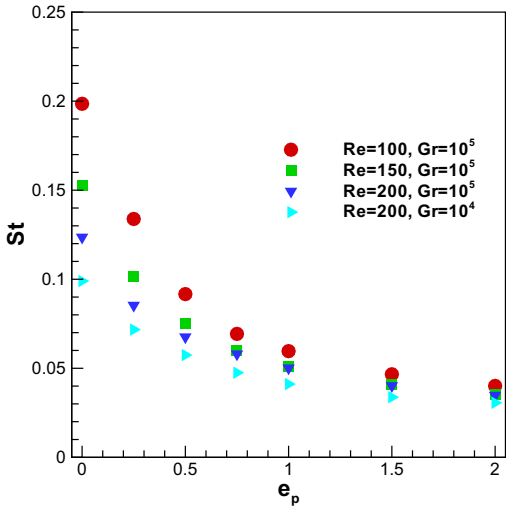

Fig. 8. Effect of porous layer thickness (e_p) on Strouhal number (St) at different Re and $Gr = 10^5$ when $Da = 10^{-5}$ and $Rc = 10$.

the lift coefficient. Fig. 8 presents the effect of the porous layer thickness on St at different values of Re and Gr. A steep jump in St from the corresponding solid cylinder case ($e_p = 0$) is observed with the introduction of the porous wrapper. The increase in porous layer thickness produces a large damping effect on the vortex shedding frequency. The Strouhal number approaches to zero asymptotically at sufficiently large value of e_p. We find that St is higher at higher values of Richardson number. This result is in agreement with the conclusion drawn by Kieft et al. [6] and Bhattacharyya et al. [18].

The time-periodic flow behind the cylinder is demonstrated with the aid of instantaneous vorticity contours and isotherms during a complete vortex shedding cycle. The results are shown in Fig. 9a–d for at Reynolds number 200 with $Gr = 10^5$ ($Ri = 0.25$) and $e_p = 0.5$. The Darcy number for the porous layer is considered to be $Da = 10^{-5}$. The time period T for vortex shedding cycle is the difference between the two successive non-dimensional times at which the lift coefficient attains its minimum value. The non-dimensional shedding period (T) is found to be 13.248 for the present set of parameter values. The fluid penetration inside the porous layer is almost negligible at this lower value of permeability, thus the outer surface of the porous layer behaves like a solid body and deflects most of the approaching fluid. Vortex sheds from the separated shear layers emerging from the outer surface of the porous layer. Part of the vorticity of the separated shear layer is diffused along the inner side of the porous layer, thus the strength of the shear layers are weaker compare to the case when the solid cylinder is considered ($e_p = 0$). The figures clearly demonstrate the alternate vortex shedding during this period. A slight strength difference is observed between the negative and positive shear layers emerging from either side of the cylinder in an alternative manner. Several authors (Kieft et al. [6], Wang et al. [19] and Bhattacharyya et al. [18]) studied the form of the vortex shedding behind a heated bluff body. Due to the buoyancy effect the vorticity is produced through the baroclinic production. The baroclinic production is positive along the upstream side of the cylinder, but negative in the downstream side. The negative baroclinic production strengthens the negative shear layer and reduces the strength of the positive shear layer emerging from the cylinder. Thus an imbalance in the strength of the opposite shear layers are created through the buoyancy effect.

The isotherm contours are presented side by side with the vorticity contours in Fig. 9a–d for $Re = 200$, $Gr = 10^5$ ($Ri = 0.25$) and $e_p = 0.5$. Isotherms form ring-like structures within the porous layer at this lower value of permeability ($Da = 10^{-5}$), which suggests that the heat transfer within the porous layer is mainly due to conduction. At the outer side of the fluid–porous interface, the heat transfer highly depends on the convection. In the clear fluid region, both vorticity and isotherms are convecting in a similar pattern. As both vorticity and thermal energy are being transported by the flow in the wake, the contour lines of vorticity and temperature have similar features. The plots of the temperature distribution show that heat is distributed within the flow field as isolated warm blobs. These warm blobs are captured within the vortex structures and convected downstream without being influenced too much by mixing with their surroundings.

4.2. Nusselt number and efficiency factor

The distribution of period-averaged local Nusselt number ($\overline{Nu}$) along the solid surface of the cylinder is presented in Fig. 10 for different values of Reynolds number when $Gr = 10^5$ and $e_p = 0.5$. The variation of period-averaged local Nusselt number along the surface of the cylinder is almost similar to the case where the porous layer is absent ($e_p = 0$). This is due to the fact that the heat transfer within the porous layer occurs mostly through conduction and hence it is governed by a linear equation. Thus the effect on heat transfer along the outer layer of the fluid–porous interface has the direct impact on the heat transfer distribution along the sur-

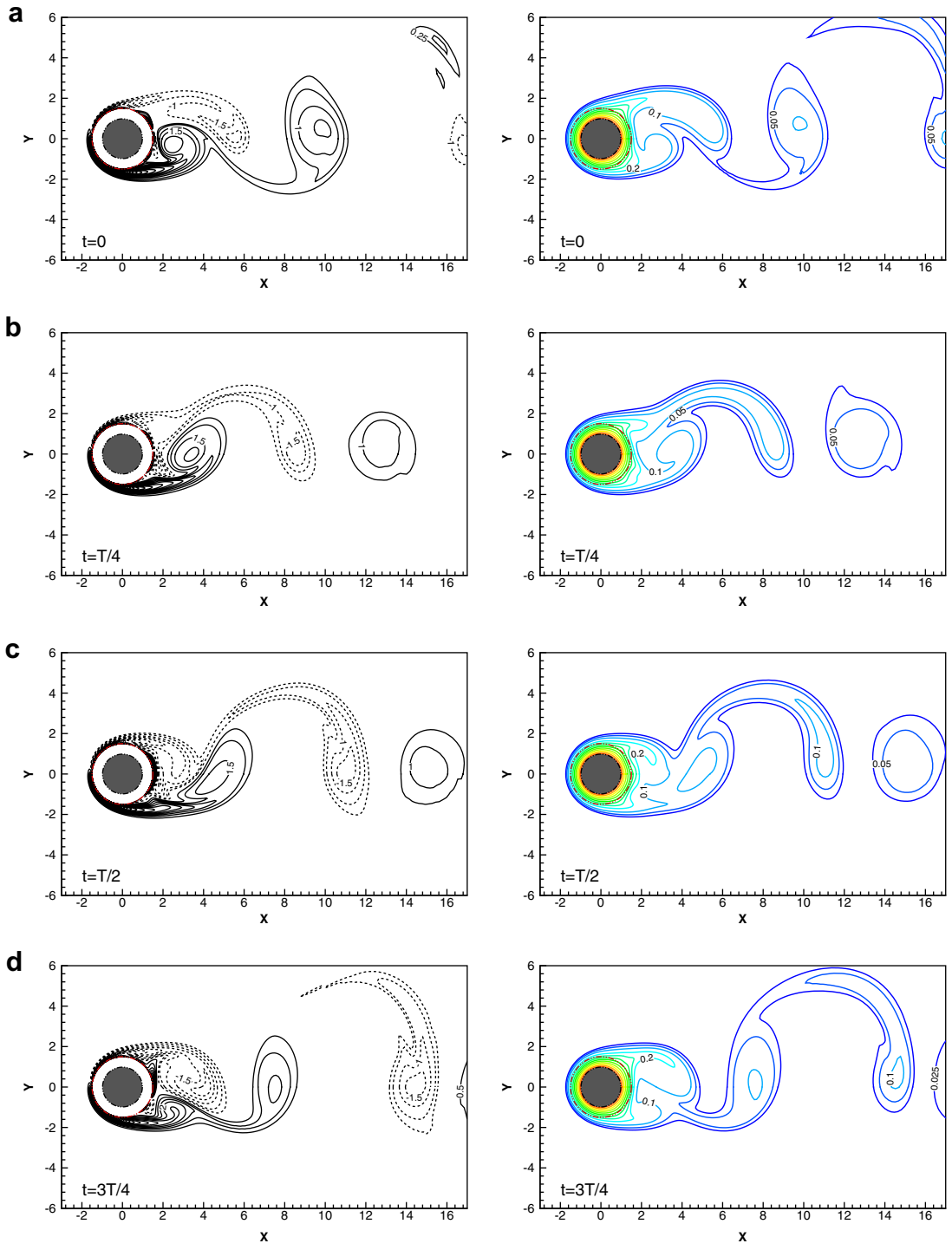

Fig. 9. Isotherm and Isovorticity contours during one shedding for $Re = 200$, $Gr = 10^5$ ($Ri = 2.5$), $Da = 10^{-5}$, $Rc = 10$ and $e_p = 0.5$, (a) $t = t_0$ ($t_0 = 126.25$, starting of the cycle); (b) $t_0 = 129.5625$ $(= t_0 + T/4)$; (c) $t = 132.875$ $(= t_0 + T/2)$; (d) $t = 136.1875$ $(= t_0 + 3T/4)$.

face of the solid cylinder for lower values of e_p. The $\overline{Nu}$ is highest at the forward stagnation point and attains local minima near the point of separation from the porous layer. The rate of heat transfer admits a minima near the rear stagnation point due to the formation of eddies in the downstream at $Re = 100$, 200. The flow is buoyancy dominated and the distribution of local Nusselt number is symmetric about the vertical axis at $Re = 40$.

The mechanism of heat transfer from the solid cylinder is mainly due to the conduction in the porous layer and the convection in fluid region. For augmentation in heat transfer, the conduction in the porous layer will have to exceed the convective heat transfer for the case of no porous layer ($e_p = 0$). Thus, the porous layer thickness and effective conductivity will have a strong influence on the heat transfer at least for the lower range of Reynolds number. We introduce the heat transfer efficiency factor, E_f, which measures the ratio between the average rate of heat transfer from a porous wrapped solid cylinder to the average rate of heat transfer from a solid cylinder with no porous layer ($E_f = \overline{Nu_{av}}/(\overline{Nu_{av}})_f$). Thus, $E_f > 1$ corresponds to heat transfer augmentation and $E_f < 1$ corresponds to insulation. The heat transfer from the

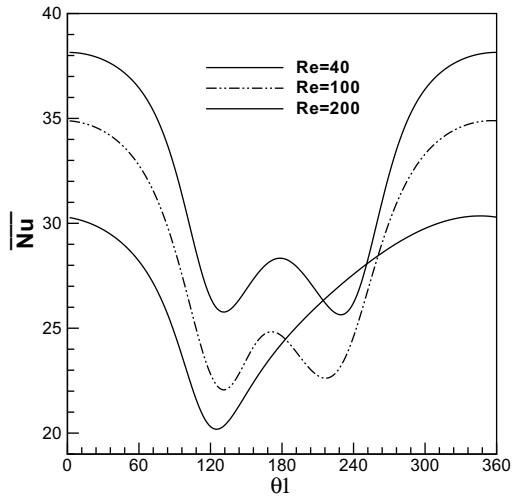

Fig. 10. Distribution of the time-averaged local Nusselt number ($\overline{Nu}$) at different Reynolds number when $Da = 10^{-5}$, $Gr = 10^5$, $e_p = 0.5$ and $Rc = 10$.

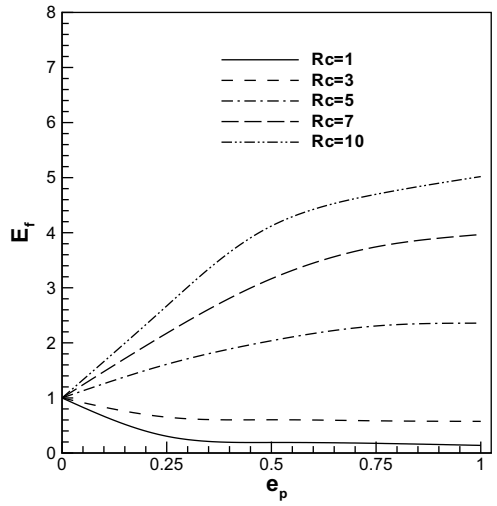

Fig. 11. Effect of porous layer thickness (e_p) on the efficiency factor (E_f) at different Rc when $Da = 10^{-5}$, $Re = 200$ and $Gr = 10^5$.

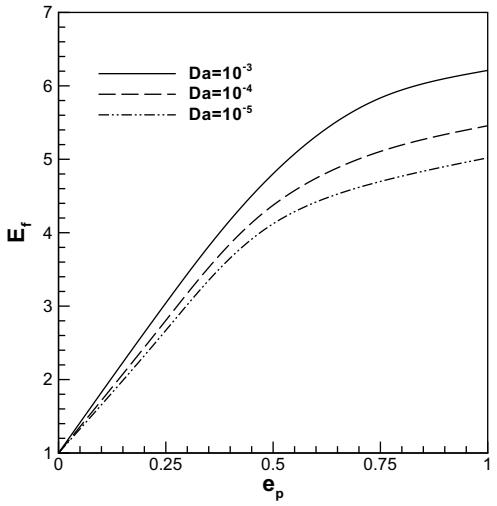

Fig. 12. Effect of porous layer thickness (e_p) on the efficiency factor (E_f) at different Da when $Re = 200$, $Gr = 10^5$ and $Rc = 10$.

cylinder coated with a porous layer depends on the permeability and thermal conductivity of the porous material. Fig. 11 depicts the effect of porous layer thickness (e_p) on the efficiency factor (E_f) at different values of the thermal conductivity ratio, Rc, when the Darcy number is 10^{-5} and $Re = 200$. Beyond a critical value of e_p, the heat transfer from the surface of the solid cylinder is invariant due to the flow along the outer side of the porous–fluid interface and thus the average Nusselt number is independent of e_p. We present the results for $Re = 200$ and $Gr = 10^5$ so that the Richardson number is 2.5. The porous layer behaves as an insulator when the thermal conductivity ratio, Rc, is below 5. The heat transfer drops substantially with the inclusion of porous layer when $Rc \leqslant 5$, till the thickness of the porous layer e_p is below 0.5. A further increase in e_p does not produce any significant change in the heat transfer. For higher value of thermal conductivity ($Rc < 5$), heat transfer is enhanced from the case of no porous layer and the heat transfer from the solid cylinder grows with the increase of porous layer thickness. Our results show that there exists a critical value of porous layer thickness beyond which the heat transfer remains invariant. This optimal thickness of porous layer for augmentation of heat transfer depends on the Reynolds number when the Darcy number, thermal conductivity and porosity are fixed. We define the critical value of e_p for which the average rate of heat transfer is maximum as the optimal thickness. We have discussed the dependence of the optimal porous layer thickness on Reynolds number, Richardson number, permeability and the thermal conductivity of the porous layer. For a highly permeable porous wrapper, the heat transfer should grow with the increase of porous layer thickness if the thermal conductivity of the material is higher.

The augmentation of heat transfer occurs when the porous wrapper is based on high thermal conductive material such as aluminum or carbon foam with high porosity. In such cases, the heat transfer is enhanced from the surface of the solid cylinder with the increase of the porous layer thickness up to a certain optimal value of the thickness. This optimal value of porous layer thickness, however, depends on the properties of foam material such as heat conductivity, porosity and permeability. The effect on efficiency factor (E_f) due to the variation of porous layer thickness is presented in Fig. 12 for different values of permeability ($Da = 10^{-3}$, 10^{-4} and 10^{-5}). The results are shown for $Re = 200$, $Gr = 10^5$ ($Ri = 2.5$) with thermal conductivity ratio as 10. For this

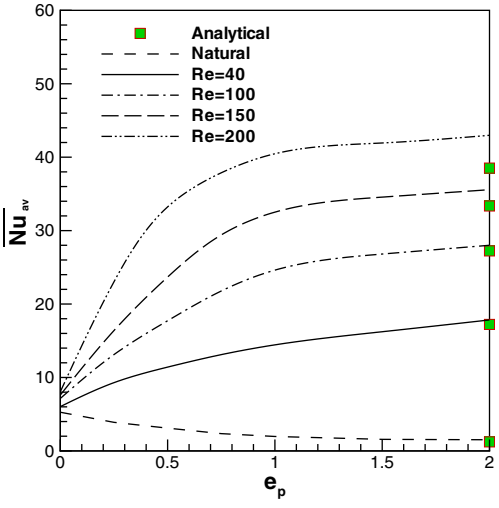

Fig. 13. Effect of porous layer thickness (e_p) on the time-averaged mean Nusselt number ($\overline{Nu_{av}}$) at different Re when $Da = 10^{-5}$, $Gr = 10^5$ and $Rc = 10$.

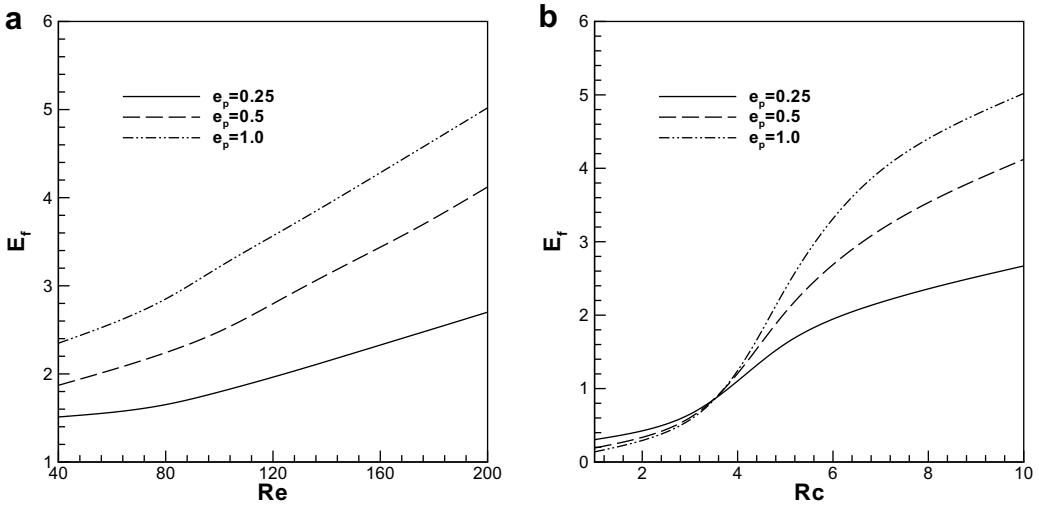

Fig. 14. Variation of the efficiency factor (E_f) at different e_p due to, (a) variation of Reynolds number; and (b) variation of the ratio of thermal conductivity. Here $Da = 10^{-5}$ and $Gr = 10^5$.

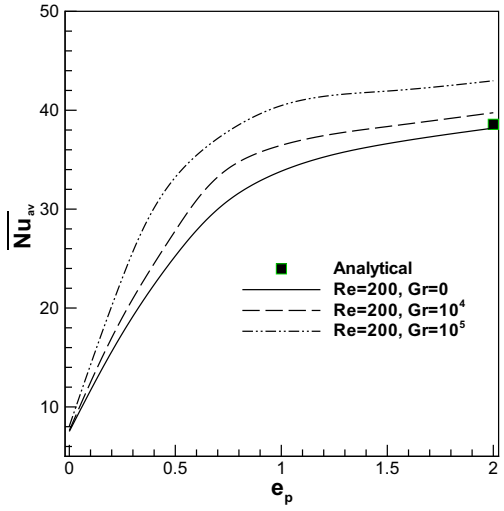

Fig. 15. Effect of porous layer thickness, e_p on the time-averaged mean Nusselt number $(\overline{Nu_{av}})$ at different Re and Gr when $Da = 10^{-5}$ and $Rc = 10$.

high value of thermal conductivity of the porous material, the heat transfer augmentation $(E_f \geqslant 1)$ occurs and the heat transfer ratio increases monotonically with the increase of e_p till an optimal value is achieved. Our results show that the increase in permeability (increase of Da) causes an increment in heat transfer from the solid cylinder at higher values of Reynolds number. The convective heat transfer within the porous layer becomes important at higher values of permeability. We find that a large heat transfer enhancement occurs with the introduction of a thin porous layer of high thermal conductivity at all values of the Darcy number considered. Our results shows that beyond a critical value of e_p, the form of the thermal boundary layer is unperturbed with the variation of the porous layer thickness. The porous layer thickness achieved its optimal value at lower range when the permeability of the material is low. Beyond the critical value of e_p for low permeability of the porous layer, the heat transfer is mainly due to conduction and the form of the thermal boundary layer along the solid cylinder become independent of how the flow field develops along the outer side of the porous–fluid interface. A similar observation for the case of natural convection is made by Saada et al. [4].

The dependence of the time average mean Nusselt number $(\overline{Nu_{av}})$ of the porous wrapped solid cylinder on the porous layer thickness at different Reynolds number is shown in Fig. 13. We have also included the case where the flow is due to natural convection. In all the results, the Darcy number is taken as 10^{-5}, $Rc = 10$ and $Gr = 10^5$. The wake is unsteady for $Re \geqslant 80$ for all value of e_p considered here. The increase in Re produces a large increment in heat transfer. Our results show that the heat transfer remains almost invariant with the increase of porous layer thickness for e_p beyond 1.5 for all $Re \geqslant 100$. For natural convection and for lower range of Re ($\leqslant$40), the optimal e_p is about 1. The porous layer with Rc = 10 (high thermal conductivity) acts as an insulator when heat transfer is due to natural convection where Ra = 72,000. It may be noted that Saada et al. [4] found an augmentation of heat transfer in natural convection for Rayleigh number as 0.125×10^8.

The average rate of heat transfer from the porous wrapped solid cylinder approaches asymptotically the corresponding value for the case where the solid cylinder is immersed within an unbounded porous media. The analytic predication for average rate of heat transfer from a solid cylinder embedded in a porous media due to natural convection [20] is

$$\overline{Nu_{av}} = 0.565Rc(Ra\,Da/Rc)^{0.5}. \tag{11}$$

Our result for Nu_{av} due to natural convection, as depicted in Fig. 13, is in close agreement with this analytical prediction. The analytical formula for the average rate of heat transfer in forced convection from a solid cylinder surrounded by an unbounded porous media [21] is

$$\overline{Nu_{av}} = 1.015Rc(Re\,Pr/Rc)^{0.5}. \tag{12}$$

This formula predicts $\overline{Nu_{av}} = 17.2251$ at Re = 40 which is quite close to our numerical result $\overline{Nu_{av}} = 17.8328$ at $e_p = 2$. At Re = 100, the analytical prediction for $\overline{Nu_{av}}$ is 27.2357 which is close to our numerical solution 28.0046 at $e_p = 2$. At Re = 200, there is a large discrepancy between the analytically predicted $\overline{Nu_{av}}$ and our computed result at $e_p = 2$. It may be noted that the analytical prediction are based on the Darcy law. Thus deviation from the analytic predictions from the computed values at large e_p become more prominent for higher values of Re.

The effect of Reynolds number on the heat transfer efficiency factor (E_f) for the lower range of porous layer thickness

($e_p = 0.25, 0.5, 1.0$) is described in Fig. 14a for a fixed value of thermal conductivity ratio ($Rc = 10$). A thin porous wrapper of high thermal conductivity produces a significant increment in heat transfer for all Re. Increase in Reynolds number produces a steady increment in heat transfer. Fig. 14b shows the variation in heat transfer ratio with the increase of thermal conductivity ratio from 1 at different values of the porous layer thickness when Reynolds number is 200. The porous wrapper acts as an insulator when thermal conductivity of the material is low (i.e., $Rc < 5$). The porous layer decreases the rate of heat losses from the cylinder. When $Rc \geqslant 5$, the value of E_f changes at a much faster rate with the change of e_p than the case where the wrapper acts as an insulator.

The effect of Grashof number on the average rate of heat transfer from the porous layer wrapped solid cylinder at different values of porous layer thickness is presented in Fig. 15. We have also included the results for forced convection case ($Gr = 0$) for comparison. Increase in Grashof number produces an increment in heat transfer as the thermal boundary layer, developed along the solid cylinder, is strong for a large Grashof number. The rate of increment in $\overline{Nu_{av}}$ is much faster with the increases of e_p when $e_p \leqslant 1$. Beyond $e_p = 1$, the $\overline{Nu_{av}}$ varies slowly with the increase of e_p and attain a constant value. Our computed solution for $\overline{Nu_{av}}$ at $e_p = 2$ agrees closely with this analytically predicted value for forced convection from a solid cylinder embedded in an unbounded porous media ($e_p \to \infty$) as given in Eq. (12).

5. Conclusion

In the present work, the augmentation of heat transfer from a solid cylinder through a porous wrapper is investigated. A thin porous wrapper made of high thermal conductivity ($Rc \geqslant 5$) can significantly enhance the heat transfer even at low permeability ($Da = 10^{-5}$). The rate of heat transfer approaches an asymptotic value, the value corresponds to $e_p \to \infty$ beyond a critical value of the porous layer thickness. This critical value of e_p is low when the heat transfer is mostly due to conduction, i.e., the permeability of the porous media is low or the Reynolds number is low. The Reynolds number and Grashof number influences the heat transfer rate substantially. The critical value of the porous layer thickness for which the heat transfer from the solid cylinder is optimum depends on the Reynolds number. The porous wrapper acts as an insulator when Rc is below 5 even at $Re = 200$, $Gr = 10^5$ when $Da = 10^{-5}$. A thin porous coating of the solid cylinder delays the vortex shedding in terms of Reynolds number. Porous coating also damps the shedding frequency when vortex shedding sets in for $Re \geqslant 80$.

Acknowledgments

The authors acknowledge the financial support received from the Council of Scientific and Industrial Research, Govt. of India through a project grant.

References

[1] M.P. Sobera, C.R. Kleijn, H.E.A. Van den Akker, P. Brasser, Convective heat and mass transfer to a cylinder sheathed by a porous layer, AIChE J. 49 (2003) 3018–3028.
[2] J.W. Paek, B.H. Kang, S.Y. Kim, J.M. Hyun, Effective thermal conductivity and permeability of almuninum foam materials, Int. J. Thermophys. 21 (2000) 453–464.
[3] A.G. Strautman, N.C. Gallego, B.E. Thompson, H. Hangan, Thermal characteristics of porous carbon foam-convection in parallels flow, Int. J. Heat Mass Transfer 49 (2006) 1991–1998.
[4] M. Ait Saada, S. Chikh, A. Campo, Natural convection around a horizontal solid cylinder wrapped with a layer of fibrous or porous material, Int. J. Heat Mass Transfer 26 (2006) 263–276.
[5] K.S. Chang, J.Y. Sa, The effect of buoyancy on vortex shedding in the near wake of a circular cylinder, J. Fluid Mech. 220 (1990) 253–266.
[6] R.N. Kieft, C.C.M. Rindt, A.A.V. Steenhoven, G.J.N. Heijst, On the wake structure behind a heated horizontal cylinder in cross-flow, J. Fluid Mech. 486 (2003) 189–211.
[7] B.D. Ingham, I. Pop (Eds.), Transport Phenomena in Porous Media, vol. II, Pergamon Press, Oxford, 1998.
[8] A. Nield, A. Bejan, Convective Heat Transfer in Porous Media, Springer, New York, NY, 1998.
[9] I. Pop, D.B. Ingham, P. Cheng, Transient natural convection in a horizontal concentric annulus filled with a porous medium, ASME J. Heat Transfer 144 (1992) 990–997.
[10] Khalil Khanafer, Ali J. Chamkha, Mixed convection with in a porous heat generating horizontal annulus, Int. J. Heat Mass Transfer 46 (2003) 1725–1735.
[11] G.S. Beavers, D.D. Joseph, Boundary condition at a naturally permeable wall, J. Fluid Mech. 30 (1967) 197–207.
[12] P. Saffman, On the boundary condition at the interface of a porous medium, Stud. Appl. Math. 50 (1971) 93–101.
[13] Beckermann, R. Viskanta, Double-diffusive convection during dendritic solidification of a binary mixture, PhysicoChem. Hydrodyn. 10 (1988) 195–203.
[14] S. Bhattacharyya, S. Dinakaran, A. Khalili, Fluid motion around and through a porous cylinder, Chem. Eng. Sci. 61 (2006) 4451–4461.
[15] C.A.J. Fletcher, Computation Technique for Fluid Dynamics, vol. 2, Springer, Berlin, 1991.
[16] R.S. Varga, Matrix Iterative Analysis, Prentice-Hall, Englewood Cliffs, NJ, 1962.
[17] H.M. Badr, Laminar combined convection from a horizontal cylinder-parallel and contra flow regime, Int. J. Heat Mass Transfer 27 (1984) 15–27.
[18] S. Bhattacharyya, D.K. Maiti, S. Dhinakaran, Influence of buoyancy on vortex shedding and heat transfer from a square cylinder in proximity to a wall, Numer. Heat Transfer A 50 (2006) 585–606.
[19] P. Wang, R. Kahawlta, D.L. Nguyen, Transient laminar natural convection from horizontal cylinder, Int. J. Heat Mass Transfer 34 (1991) 1429–1442.
[20] P. Cheng, The influence of lateral mass flux on free convection boundary layers in a saturated porous medium, Int. J. Heat Mass Transfer 20 (1977) 206.
[21] J. Thevenin, D. Sadaoui, About enhancement of heat transfer over a circular cylinder embedded in a porous medium, Int. Commun. Heat Mass Transfer 22 (1995) 295–304.